Received: 27 May 2019 | Accepted: 11 July 2019

DOI: 10.1002/ces2.10017

International Journal of Ceramic Engineering & Science

ORIGINAL ARTICLE

Superior performing nano-enabled metal oxide varistors

Daniel Q. Tan

Technion Israel Institute of Technology and Guangdong Technion Israel Institute of Technology, Shantou, China

Correspondence
Daniel Q. Tan, Technion Israel Institute of Technology and Guangdong Technion Israel Institute of Technology, 241 Daxue Rd, Jinping District, Shantou, Guangdong 515063, China.
Email: Daniel.tan@gtiit.edu.cn

Funding information
Technion-Israel Institute of Technology startup

Abstract

Commercial metal oxide varistor devices are subject to nonuniformity, defects and coarse grain size, low working voltage, high leakage current, and mechanical cracking issues. This work tempted to make use of nanopowders and alternative sintering processes to achieve uniform microstructure and superior varistor performance. These nano-enabled compositions exhibit lower sintering temperatures (650-1050°C), smaller grain sizes (0.5-2 μm), enhanced nonlinear coefficient (30-130) in DC I-V characteristics, higher varistor voltages (240-2500 V/mm), and low leakage current (<1 μA/cm^2). Conventional sintering offers highest nonlinearity. Spark plasma sintering and microwave sintering techniques show advantages in reducing grain sizes and sintering temperatures. Spark plasma sintering is particularly effective in achieving better varistor performance for the nano-enabled MOV compositions after a post-SPS sintering for sufficient oxygen diffusion. Microwave sintering needs higher sintering temperatures and additional research for the nano-enabled MOV compositions to offer equivalent electrical properties.

KEYWORDS

nanoparticles, sintering, varistor, zinc oxide

1 | INTRODUCTION

Over voltage is a common phenomenon in various businesses such as wireless communication, computing systems, automotive, entertainment, industrial equipment, and military systems. Even the best-designed electric system is subject to over voltages. Therefore, various surge protection devices such as surge suppressors (e.g., circuit breakers or fuses, attenuating transients) and surge diverters (e.g, varistor, diverting the surge away from the protected device) are used in the electric systems to suppress it.[1] Among them, metal oxide varistors (MOV) have been the number one surge protection component since late 1970s.[2,3] Comparatively, MOVs have higher nonlinearity (α value), fast voltage clamping response, and transient surge suppression for wide applications.

Metal oxide varistors are a grain boundary-controlled device, in which the double Schottky barrier has a breakdown voltage of 2-3.6 V per grain boundary.[4,5] The phase composition and thickness of grain boundary, the microstructure uniformity and porosity of a MOV compound directly affect its voltage clamping performance. For example, sintering processes (in air, reduced atmosphere, oxidation) and operating temperature of varistors were found to result in nonlinear properties due to the change of oxidation state of grain boundaries.[6–10] Yet, the conventional thermal sintering process (TSP) is not capable of reaching a full density in a commercial MOV as shown in Figure 1. In addition, sintering at temperatures higher than 1100°C results in nonuniform microstructure with an average grain size of >7 μm, lower α value (<50), low varistor (working) voltage (<200 V/mm), and higher leakage current (>10 μA/cm^2). Researchers

attempted nanopowders as the precursors to lower sintering temperatures expecting better sinterability, capable of cofiring with noble metals, higher homogeneity, and electrical properties.[11–18] However, most of the efforts were made either on ZnO-only or on ZnO-Bi_2O_3 only, which are not genuine varistor compositions with commercial usefulness. Only limited efforts are carried out on the multiple-ingredient ZnO varistor compositions. Although good results were obtained, there remains necessity to further decrease grain size below 1 μm, sintering temperature below 950°C, leakage current density below 1 μA/cm^2, and to increase nonlinearity above 60, and working voltage above 1 kV/mm.[17,18]

On the other hand, processing methods directly affect the microstructure and properties of varistor compounds (Figure 2). Conventional pressureless sintering, hot pressing (HP), spark plasma sintering (SPS), and microwave sintering (MWS) were utilized to sinter varistors more or less. SPS and MWS, however, were not well utilized for MOVs in spite of their advantages on lower sintering temperatures and shorter sintering time.[19–23] For example, Lin et al[24] achieved dense ZnO-only compacts using SPS under 850°C without showing varistor characteristics. Macary et al.[25] achieved 0.5 μm grain size in ZnO-Bi_2O_3 compacts using SPS technique at 600-800°C, but failed to show a meaningful varistor characteristics. Working with nano-sized ZnO-Bi_2O_3-based multiple-ingredient compositions, Beynet et al.[26] ended up at coarser grain size (3-8 μm) after SPS at 600-870°C, yet delivered electrical properties far from useful nonlinear characteristics. Lin et al[21] only achieved decent varistor characteristics using micron-sized ZnO powders and microwave sintering at 1100°C, which did not leverage the advantages of microwave technique very much. In fact, no reports were found applying SPS and MWS techniques on nanopowder-based varistors to demonstrate useful nonohmic varistor characteristics with high nonlinearity. How good microstructure and electrical properties can be achieved in the meaningful compositions using this field-assisted sintering process should be found out. In this work, we focused on the several meaningful compositions made of nanopowders and investigate their microstructures and electrical properties using low temperature conventional sintering, SPS, and MWS processes. We will demonstrate the superior varistor performance and the capability of these sintering processes.

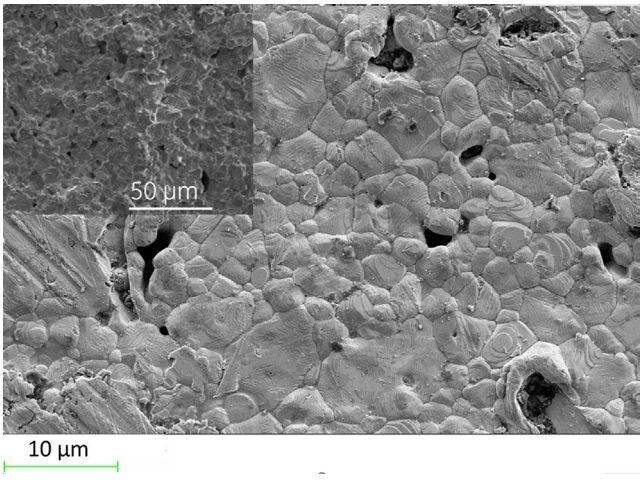

FIGURE 1 SEM image of a commercial MOV sintered at high temperatures

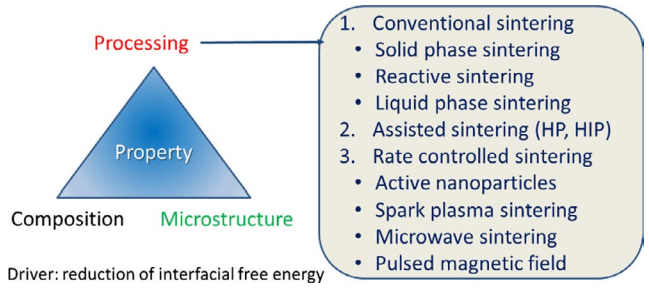

FIGURE 2 Relationship between composition, processing, structure and property, and ceramic sintering methods

2 | EXPERIMENTAL

All oxide ingredients are commercially available from common chemical suppliers such as Horsehead Corporation, Nanostructured and Amorphous Materials Inc., Alpha Aesar, Inc., Sigma-Aldrich, and Spectrum Chemical Mfg. Corp. A mixture is formed from zinc oxide, and additives selected from cobalt, antimony, nickel, and chromium oxide nanopowders as well as bismuth, silicon, and manganese nanopowders in certain ratios. The MOV compositions being studied in this work were based on the previously developed compositions that were characterized for meaningful varistor characteristics.[17,18] They are labeled as MOV-a, MOV-b, MOV-c (this Lab), and MOV-L (commercial) as shown in Table 1. The major ingredients comprise nano-sized ZnO, Sb_2O_3, Bi_2O_3, and other oxide additives.

The MOV samples are prepared by mixing, calcining, ball milling, and sintering. The precursor mixture is milled in a ball mill for about 6 hours in a ratio materials: ball:isopropyl alcohol = 1:5:2 to form a slurry. The slurry is dried at 100°C. The dried powder is sieved and calcined at 550°C for about 2 hours. The calcined powder is then ball milled for about 4 hours. The powder is then pressed into pellets that are about 25 cm in diameter and 1.5 mm in thickness with a force of about 10 000 pounds for about 1 minute. The pellets are sintered at temperatures from about 850-1050°C.

The SPS unit passes a pulsed DC current through a powder sample contained in a cylindrical graphite punch and dies set while applying a constant pressure. The graphite die used is 30 mm tall, with a 30 mm outer diameter

TABLE 1 Metal oxide varistor compositions and powder information

Sample name	ZnO/nano	Bi_2O_3/nano	Other additives/nano	Remark
MOV-a	94.0%	0.5%	Multiple	This Lab
MOV-b	90.9%	3.0%	Multiple	This Lab
MOV-c	94.7%	3.0%	Multiple	This Lab
MOV-L	<90.0%/micron	>2.0%/micron	Multiple/micron	Commercial

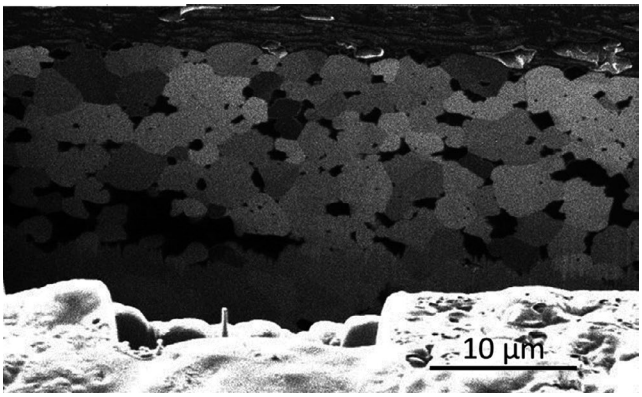

FIGURE 3 FIB-SEM image of a MOV-a sample after sintering at 1000°C for 2 h

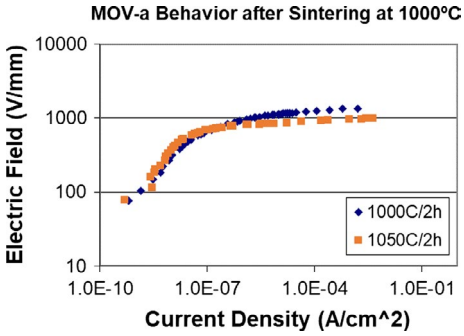

FIGURE 4 Electrical properties of a MOV-a sample after sintering at 1000 and 1050°C

(OD) and a 15.35 mm inner diameter. A graphite disk is placed on top of the ZnO-based powder followed by the insertion of a top punch. Graphite spacers are placed on the bottom electrode of the SPS unit and centered below the top electrode. The control thermal couple is inserted into the side hole in the center of the die. A clamping force of 3.1 kN is applied to the spacers and the die/punch set. The pressure on the punch and die is increased to 40 MPa. The sample is heated to the sintering temperature for the given MOV powder. The pressure is increased to 60 MPa when the sample has reached its sintering temperature for the specified time.

Microwave sintering of MOV compositions was conducted in a 2.45 GHz microwave furnace of 6 kW in air. The samples loaded in a thermal insulation package received microwave power with proper temperature uniformity that is monitored by an optical pyrometer.

Scanning electron microscopy (SEM) imaging was done using a Zeiss Supra 55VP to show the surface microstructure of MOV components. Focal ion beam (FIB) was used to show the cross-sectional microstructure of MOV components. The DC I-V characteristics were obtained from the measurements of resistance of MOV using an electrical circuit.

3 | RESULTS AND DISCUSSIONS

Conventional sintering using nanopowder precursors, SPS, and MWS sintering methods are utilized to investigate their effectiveness on microstructural development and varistor performance improvement.

3.1 | Conventional sintering using nanopowder precursors

3.1.1 | Nanopowder effect

For different compositions such as MOV-a, lower temperatures are found also feasible for reaching high density. Figure 3 shows the cross-sectional image of the MOV-a sample sintered at 1000°C using a FIB-SEM technique. Comparing with a commercial MOV compound having grain sizes up to 15 μm (Figure 1), the nano-enabled MOV-a has a uniform microstructure with an average grain size being ~3 μm. The electrical performance as shown in Figure 4 also exhibits the advantage of I-V characteristics comparing with the commercial MOV that uses micro-sized oxide powders as precursors. The working voltage of the MOV-a reaches ~0.95 kV/mm, about five times of a commercial MOV's. The nonlinearity value is 20. Sintering at higher temperatures (≥1050°C) does not decrease the working voltage much but increase the nonlinearity to 32. This again shows the advantages of using nanopowder precursors for finer microstructures and varistor behavior in different MOV compositions.

3.1.2 | Sintering additive effect

Adding more sintering additives like 3% Bi_2O_3 further lowered the sintering temperature down to 850°C as previously reported, which is associated with low-melting eutectic

formation.[17,18,27] Recently, we found that sintering MOV-c at higher temperatures (1050°C) still maintains the varistor characteristics with a high nonlinearity of 79 and working electric field of 315 V/mm, which are better than commercial MOVs that are sintered at 1200°C (Figure 5). The SEM image shows the grain size being no more than 5 microns and the grain boundary phase being uniformly dispersed globally as shown in Figure 6. According to prior grain boundary junction mechanism, the Bi-rich phase developed at the grain boundaries increases the interface acceptor state density and the charge depletion layer width.[4,6] As result, the varistor voltage increases besides the increased number of junctions per unit volume of varistor.

3.2 | Spark plasma sintering at lower temperatures

Spark plasma sintering as a typical rate-controlled sintering process functions well with an assistance of a pulse electrical current passing through the compacted powders under a pressure.[28] Because of local heating inside the compact, the interfacial spaces can be eliminated more effectively at relatively low sintering temperatures.[29] As a result, we recently used SPS technique to sinter nano-enabled MOV-a compositions so as to further derive finer microstructure against those from conventional sintering.

3.2.1 | MOV with nanostructure

When the sintering temperature of MOV-a is below 650°C, no high density (<90%) can be reached. When the sintering occurs at above 650°C for 5-15 minutes, high density can be obtained and the powders in the graphite die are converted into dark pellets due to oxygen deficiency as shown in Figure 7A. The microstructure of SPS sample was polished and prepared for the subsequent inspection using SEM and FIB. Figure 7B and C shows the surface fractured image and cross-sectional image, respectively. The grain size is in the range of 0.2-0.6 μm.

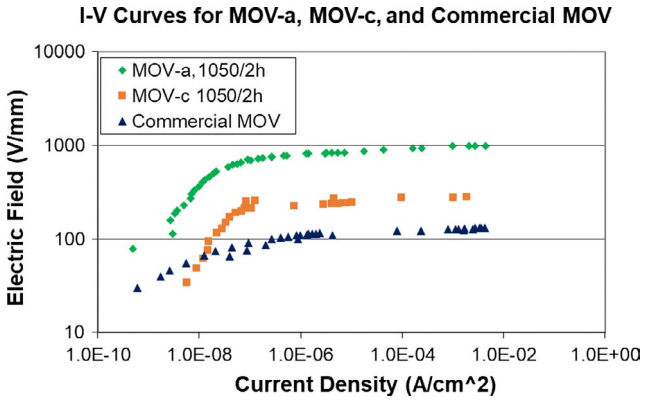

FIGURE 5 Electrical properties of three nano-enabled MOV compositions and commercial MOVs

3.2.2 | Electrical property

In order to convert the electrically conducting samples to varistor characteristics, all SPS samples were subsequently oxidized in air environment. The oxidation temperature ranges from 550-800°C, and the dwelling time is 1-5 hours. Figure 8A shows the I-V characteristics of a MOV-c composition upon oxidation. The oxidation process is very effective to convert a conducting SPS samples to varistor characteristic performance with a higher nonlinearity (52). This indicates the diffusion of oxygen into grain boundaries to form thick grain boundary junctions as explained in the literature.[16–18,30] The insufficient oxygen diffusion in the dense MOV compacts also explains the appearance of high leakage current at low voltages.

In order to reach thorough and uniform oxygen diffusion, some MOV samples were only partially compacted using SPS technique, and a subsequent sintering in air was carried out. The I-V characteristics exhibit differently for different starting density after SPS process as shown in Figure 8B. Highly densified MOV-1 only exhibited lower nonlinearity even after further sintering at 900°C for 2 hours in air. A lower density SPS sample exhibits better varistor characteristics after subsequent sintering in air. When a SPS sample is only 45% dense, further sintering at 950°C for 2 hours results in the high nonlinearity (50), low leakage current, and the working electric field. The highest working electric field was achieved for this composition (>2 kV/mm) comparing with the conventionally sintered MOV-a (0.95 kV/mm). The response time of the varistor is also faster and the voltage quickly reaches its flat plateau.

3.3 | Microwave sintering for shorter time

Microwave sintering was known to be a noncontact method and to provide heat flow from inside to outside.[31] For

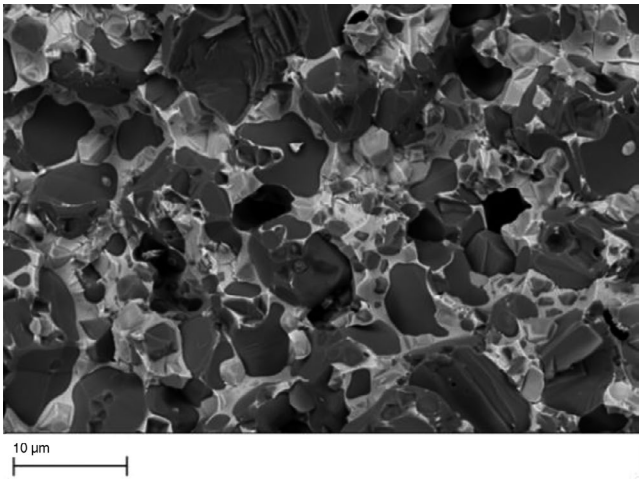

FIGURE 6 SEM image of the fracture surface of a MOV-c after sintering 1050°C for 2 h

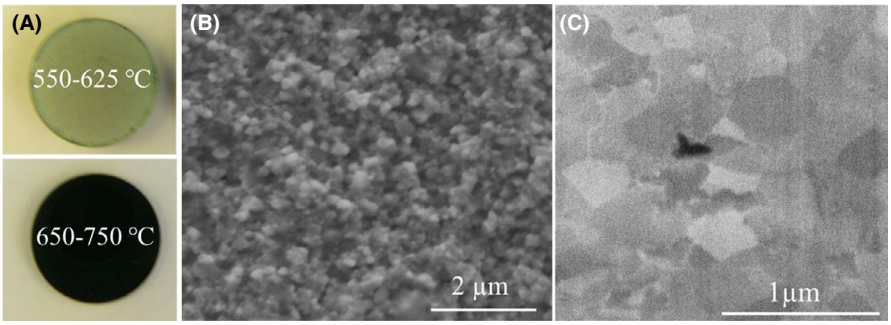

FIGURE 7 A, Images of MOV-a compacts after SPS processes at different temperatures, B, fracture surface image and C, cross-sectional image of FIB-SEM of MOV-a sintered at 650°C for 10 min

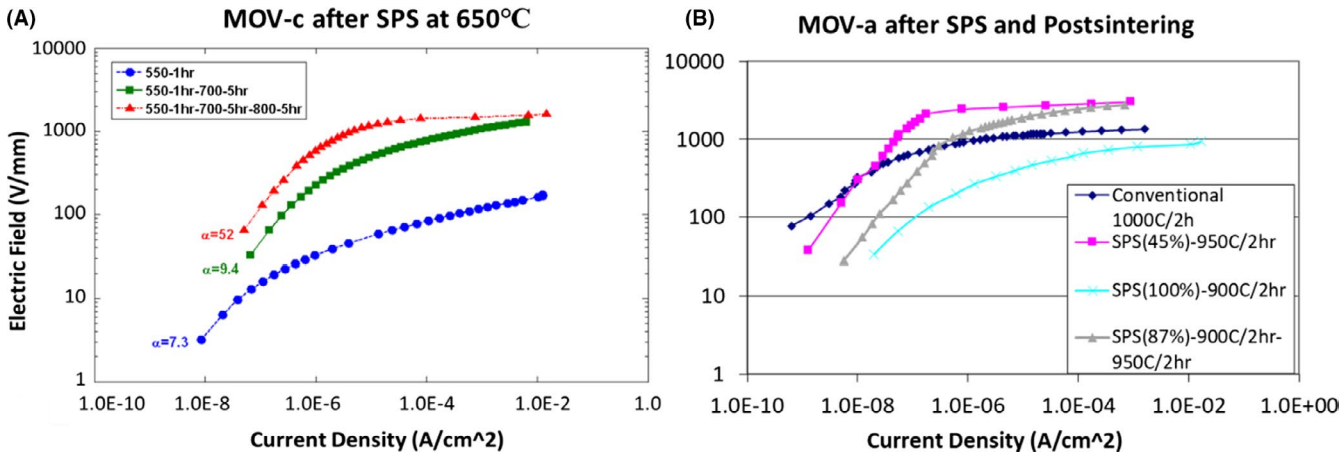

FIGURE 8 Electrical properties of MOV-c after SPS and oxidation at various temperatures (A), and MOV-a after SPS and subsequent pressureless sintering in air at various temperatures (B)

electrically conductive materials such as ZnO, power penetration can be quite deep because of the large skin depth of ZnO particles as demonstrated before.[32,33] For nano-sized ZnO smaller than the skin depth, a uniform heating can be expected. Sintering temperature was reduced from 1250 to 1100°C, and much shorter time was used for densification. When it comes to MOV compositions that containing grain boundary phases and nonconductive nano-sized additives, limited information was known. Therefore, we applied microwave sintering technique to MOV-a compositions expecting to understand more about its sintered microstructure and varistor properties.

3.3.1 | Microstructure of nano-enabled MOVs

Sintering of MOV-a pellets was carried at temperature from 750 to 1000°C. The microwave power was provided for 5-20 minutes in various experiments. Figure 9 shows the fracture surface images of three MOV compositions sintered at four different temperatures. The microstructures show limited grain growth but broad grain size distribution with increasing the sintering temperature. At 750°C, the average grain size of MOV-a is about 0.5 micron and the density is relatively low. At 950 or 1000°C, no considerable grain growth occurs and grain size appears in the range of 0.5-2 micron. The grain boundary phase (white areas) appears to be conformally networked at the grain boundaries forming a typical MOV microstructure junctions. Similar microstructures were observed for other two MOV compositions that were sintered at 800-850°C. For example, when sintering MOV-c at 850°C, the grain size is about 1.5 micron and density is moderately high. In comparison with commercial MOV, the grain size is much smaller providing more supply of barrier junctions for varistor performance. However, the unbalanced grain growth can be related to the nonconducting oxide additives that absorbs less microwave power during the sintering.

3.3.2 | Electrical property

The varistor characteristics of the microwave-sintered samples were tested using the steady-state current test setup. Figure 10 shows that the I-V curves for the MOV-a sample after microwave sintering at 950°C for 5 minutes and conventional sintering at 1000°C for 2 hours. The microwave sintering does not result in a high nonlinearity[10] and lower leakage current comparing with that by the conventional sintering. This may be related to the broad grain size distribution and unfavorable grain boundary junction.

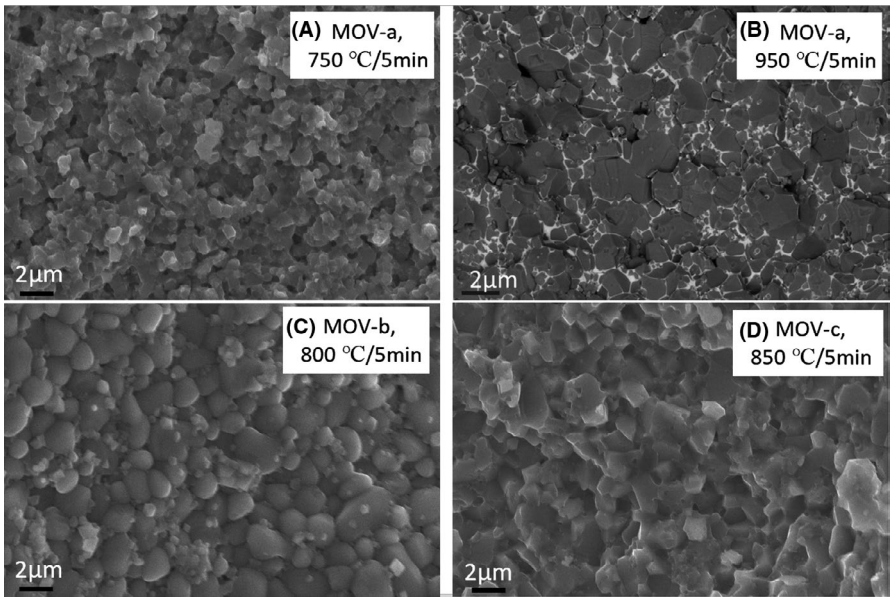

FIGURE 9 SEM images of fracture surface of MOVs after SPS sintering at various temperatures. A, MOV-a at 750°C, B, MOV-a at 950°C, C, MOV-b at 800°C, and D, MOV-c at 850°C

3.4 | Comparison of different sintering techniques

Multiple additives are used to enhance the grain boundary barrier and thus the varistor voltage or electric field. Among various oxide additives (CoO, Cr_3O_4, Bi_2O_3, Sb_2O_3, Mn_2O_3, NiO, SnO_2, SiO_2, and Al_2O_3), Bi_2O_3, Sb_2O_3, and NiO have critical roles not only for grain boundary junctions, but also for grain growth restriction and sintering temperature reduction. They can sensitively change the sintering process, microstructure, and electrical properties. Use of nanopowders and conventional sintering has resulted in uniform microstructure with smaller average grain size (1-3 μm) and higher nonlinearity (60-130). However, their effect on reaching microstructure below 1 μm is limited if sintering temperature is not lowered than 900°C.[18] Grain sizes of 0.3-1 μm become possible using SPS technique as shown in Figure 11. The shaded bars show the range of sintering temperatures for various MOV compositions. The advantages are attributed to the quick elimination of free surface spaces and retarded grain boundary diffusion due to lowered sintering temperatures. In spite of lower α value, the smaller grain sizes in SPS samples provide the increased number of grain boundaries, which is beneficial for higher working voltage and longer life expectation for MOV. Microwave technique turned out not performing as well as other two techniques in terms of nano-enabled MOV performance. This result is somewhat in agreement with that of MOVs made of micron-sized powder, which exhibits higher nonlinearity but also high leakage current, large grain size distribution in micron range after microwave sintering at 1000-1100°C.[34] This may be related to the use of different compositions and nonuniform electrical conductivity of the oxide mixture. Comparing with conductive ZnO, many other additives are nonconductive and their microwave energy absorption is limited, and the internal heating rate in those regions is less than ZnO region. Inhomogeneous heating and grain growth are then resulted inside the pellets. A recent interesting progress in sintering techniques was the

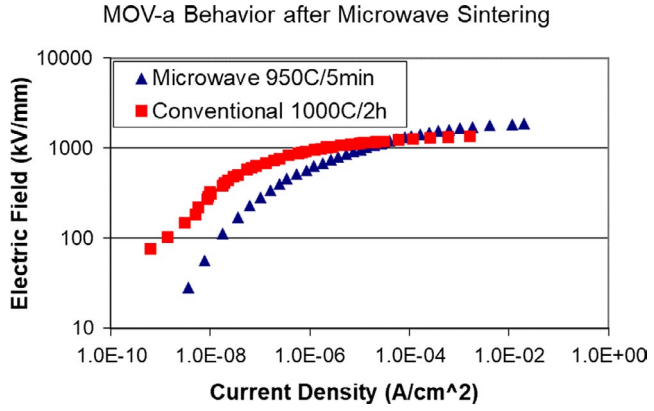

FIGURE 10 Electrical properties of a MOV-a sample after MWS and conventional sintering

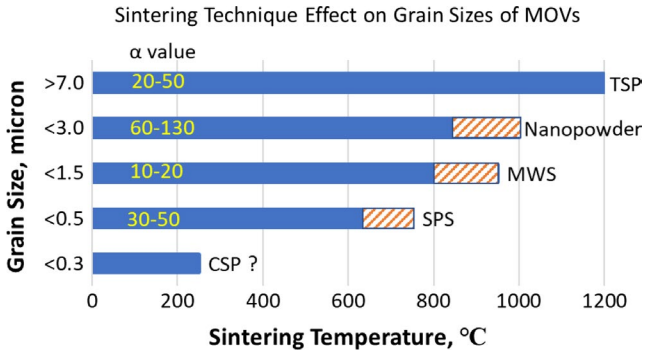

FIGURE 11 Effect of various sintering techniques on the grain size and properties of MOVs

cold sintering process (CSP).[35] Is it possible to use it to further lower the sintering temperature below 250°C and grain size of below 300 nm? This could be an interesting subject of investigation for MOVs.

4 | CONCLUSIONS

Nano-oxide powders were used as the precursors for several MOV compositions, and superior overall varistor performance was achieved in MOV compositions developed at this laboratory. The conventional sintering process gives rise to homogeneous microstructures, grain size below 3 μm, sintering temperatures 850-1050°C, nonlinearity higher than 60, leakage current of $<10^{-7}$ A/cm^2, and working voltage of >5 times of commercial MOVs.

Superior performance was also achieved using field-assisted SPS process and nano-enabled MOV compositions. Submicron grain sizes (0.3-1.5 μm), lower sintering temperature (650-750°C), and higher varistor voltage (2 kV/mm) were shown for a MOV-a composition. The process comprising SPS partial sintering and the subsequent sintering renders more favorable microstructure and varistor performance.

Microwave sintering delivers relatively smaller grain size in shorter sintering time at temperatures of 800-950°C; however, the electrical properties of MOVs being used in this work are not equally good. The internal heating mechanism absorbing microwave power may subject to the nonuniformity issue at conductive ZnO grains and other nonconductive grain boundary phases.

ACKNOWLEDGMENTS

This research was supported by the start-up fund of Guangdong Technion Israel Institute of Technology. The discussion and support of my colleagues and microstructure imaging services are acknowledged.

ORCID

Daniel Q. Tan https://orcid.org/0000-0002-2282-2000

REFERENCES

1. DOE Office of Science. Technology And Applied R&D Needs For Materials Under Extreme Environments Resource Document for the Workshop on Basic Research Needs for Materials Under Extreme Environments. 2007.
2. Levinson LM (editor). Advances in varistor technology. In: Ceramic Transactions. Westerville, OH: American Ceramic Society, 1989; 3.
3. Wang H, Bartkowiak M, Modine FA, Dinwiddie RB, Boatner LA, Mahan GD. Nonuniform heating in zinc oxide varistors studied by infrared imaging and computer simulation. J Am Ceram Soc. 1998;81(8):2013–2022.
4. Clarke DK. Varistor ceramics. Am Ceram Soc. 1999;82(3):485–502.
5. Gupta TK, Carlson WG. Barrier voltage and its effect on stability of ZnO varistor. J Appl Phys. 1982;53(11):7401–7409.
6. Fu QY, Chen T, Ye XJ, Chen PY, Liu Y, Gao C, et al. ZnO varistor ceramics prepared by the reduction–reoxidation method. J Eur Ceram Soc. 2015;35:3025–3031.
7. Sonder E, Austin MM, Kinser DL. Effect of oxidizing and reducing atmospheres at elevated temperatures on the electrical properties of zinc oxide varistors. J Appl Phys. 1983;54(6):3566–3572.
8. Stucki F, Greuter F. Key role of oxygen at zinc oxide varistor grain bound-aries. Appl Phys Lett. 1990;57(5):446–448.
9. Ramırez MA, Simoes AZ, Bueno PR, Marquez MA, Orlandi MO, Varela JA. Importance of oxygen atmosphere to recover the ZnO-based varistors properties. J Mater Sci. 2006;41(19):6221–6227.
10. Alim MA, Li ST, Liu FY, Cheng PF. Electrical barriers in the ZnO varistor grain boundaries. Phys Status Solidi A. 2006;203(2):410–427.
11. Hwang CC, Wu TY. ZnO Based Varistor Derived from Nano ZnO Powders and Ultrafine Dopants. Mater Sci Eng, B, 2004;111:197–206.
12. Roy PK. Synthesis of nano Zno powder and study of its varistor behavior at different temperatures. J Mater Sci Res. 2012;1(4):28–34.
13. Pillai SC, Kelly JM, McCormack DE, O'Brien P, Ramesh R. The effect of processing conditions on varistors prepared from nanocrystalline ZnO. J Mater Chem. 2003;13:2586–2590.
14. Hembram K, Sivaprahasam D, Rao TN. Combustion synthesis of doped nanocrystalline ZnO powders for varistors applications. J Eur Ceram Soc. 2011;31:1905–1913.
15. Sedghia A, Noorib NR. Comparison of electrical properties of zinc oxide varistors manufactured from micro and nano ZnO powder. J Ceram Process Res. 2011;12(6):752–755.
16. Dosch RG, Tuttle BA, Brooks RA. Chemical preparation and properties of high-field zinc oxide Varistors. J Mater Res. 1986;1(1):90–99.
17. Tan DQ, Younsi K, Zhou YN, Irwin PC, Cao Y. Nano-enabled Metal Oxide Varistors. IEEE Trans Dielectr Electr Insul. 2009;16(4):934–939.
18. Tan DQ, Irwin PC, Younsi K. Electronic device and method. US Patent 8,217,751, July. 2012.
19. Snow GS, White SS, Cooper RA, Armijo JR. Characterization of high field varistors in the system ZnO-CoO-PbO-Bi_2O3. Am Ceram Soc Bull, 1980;59(6):617–622.
20. Takemura T, Kobayashi M, Takada Y, Sato K. Effects of Bismuth Sesquioxide on the Characteristics of ZnO Varistors. J Am Ceram Soc. 1986;69(5):430–436.
21. Tilley BS, Kriegsmann GA. In microwaves: theory and application in materials processing V. In: Clark DR, Bonner JP, Lewis DA, editors. Ceramic Transaction. Westerville, OH: The American Ceramic Society, 2001; 111, 3.
22. Agrawal D, Raghavendra R, Vaidhyanathan B. US patent No. 6,399,012. 2002.
23. Lin IN, Lee WC, Liu KS, Cheng HF, Wu MW. On the microwave sintering technology for improving the properties of semiconducting electronic ceramics. J Eur Ceram Soc. 2005;21:2085–2088.
24. Lin DB, Fan LC, Shi Y, Xie JJ, Lei F, Ren DD. Elaboration of translucent ZnO ceramics by spark plasma sintering under low temperature. Opt Mater. 2017;71:151e156.
25. Macary LS, Kahn ML, Estourne`s C, Fau P, Tre´mouilles D, Bafleur M, et al. Size effect on properties of varistors made from

zinc oxide nanoparticles through low temperature spark plasma sintering. Adv Funct Mater. 2009;19:1775–1783.
26. Beynet Y, Izoulet A, Guillemet-Fritsch S, Chevallier G, Bley V, Pérel T, et al. ZnO-based varistors prepared by spark plasma sintering. J Eur Ceram Soc. 2015;35:1199–1208.
27. Kang XY, Tu MJ, Zhang M, Wang TD. Microstructure and electrical properties of doped ZnO varistor. Solid State Phenom. 2004;100:127–132.
28. Bernik S, Bernard J, Daneu N, Recenik A. Microstructure development in low-antimony oxide-doped zinc oxide ceramics. J Am Ceram Soc. 2007;90(10):3239–3247.
29. Guillon O, Gonzalez-Julian J, Dargatz B, Kessel T, Schierning G, Rathel J, et al. Field-Assisted Sintering Technology/Spark Plasma Sintering: Mechanisms, Materials, and Technology Developments. Adv Eng Mater. 2014;16(7):830–849.
30. Saadeldin MM, Desouky OA, Ibrahim K, Khalil GE, Helali MY. Investigation of structural and electrical properties of ZnO varistor samples doped with different additives. NRIAG J Astronomy Geophys. 2018;7:201–207.
31. Goto T. Applications of Spark Plasma Sintering, 2nd International school-seminar "Perspective technology of materials consolidation with electromagnetic fields". 1st Russia-Japan SPS Workshop Moscow 2013; Russia, May 20
32. Cherian K, Cheng J. Advances in high-temperature microwave processing, Industrial Heating 2007; August, 79–82.
33. Agrawal D. Microwave sintering of ceramics composites and metallic materials, and melting of glasses. Trans Indian Ceram Soc. 2014;65:129.
34. Cong L, Zheng X, Hu P, Sun DF. Bi2O3 Vaporization in Microwave-Sintered ZnO Varistors. J Am Ceram Soc. 2007;90(9):2791–2794.
35. Guo J, Baker AL, Guo H, Lanagan M, Randall CA. A new era for ceramic packaging and microwave device development. J Am Ceram Soc. 2017;100:669–677.

How to cite this article: Tan DQ. Superior performing nano-enabled metal oxide varistors. *Int J Ceramic Eng Sci*. 2019;1:136–143. https://doi.org/10.1002/ces2.10017